Chemical Characterization and Quantification of Circulating Intact PTH and PTH Fragments by High-Resolution Mass Spectrometry in Chronic Renal Failure

Kittrawee Kritmetapak[a,b], **Louis A. Losbanos**[a], **Jolaine M. Hines**[c], **Katherine L. O'Grady**[c], **Candice Z. Ulmer**[d], **Hubert W. Vesper**[d], **Felicity T. Enders**[e], **Ravinder J. Singh**[f,*], **Rajiv Kumar**[a,g,*]

[a]Division of Nephrology and Hypertension, Department of Internal Medicine, Mayo Clinic, Rochester, MN, USA [b]Division of Nephrology, Department of Medicine, Faculty of Medicine, Khon Kaen University, Khon Kaen, Thailand [c]Immunochemical Core Laboratory, Mayo Clinic, Rochester, MN, USA [d]Centers for Disease Control and Prevention, Atlanta, GA, USA [e]Division of Biomedical Statistics and Informatics, Department of Health Sciences Research, Mayo Clinic, Rochester, MN, USA [f]Department of Laboratory Medicine and Pathology, Mayo Clinic, Rochester, MN, USA [g]Department of Biochemistry and Molecular Biology, Mayo Clinic, Rochester, MN, USA

*Address correspondence to: R.K. at Medical Sciences 1-120, Division of Nephrology and Hypertension, 200 1st Street SW, Rochester, MN 55905. Tel 507-284-0020; rkumar@mayo.edu. R.J.S. at Clinical Mass Spectrometry Laboratory, Department of Laboratory Medicine and Pathology, Superior Drive, Rochester, MN 55905, USA. Telephone: 507-255-3952; Singh.Ravinder@mayo.edu.

Publisher's Disclaimer: Disclaimer: The findings and conclusions in this report are those of the authors and do not necessarily represent the views of the Centers for Disease Control and Prevention.

Supplemental Material
Supplemental material is available at *Clinical Chemistry* online.

Abstract

BACKGROUND: The precise concentrations of full-length parathyroid hormone (PTH1–84) and the identity and concentrations of PTH fragments in patients with various stages of chronic renal failure are unknown.

METHODS: We developed a liquid chromatography-high resolution mass spectrometry (LC-HRMS) method to characterize and quantify PTH1–84 and PTH fragments in serum of 221 patients with progressive renal dysfunction. Following capture by matrix-bound amino-terminal or carboxyl-terminal region-specific antibodies and elution from matrix, PTH1–84 and PTH fragments were identified and quantitated using LC-HRMS. PTH was simultaneously measured using an intact PTH (iPTH) immunoassay.

RESULTS: Full-length PTH1–84 and 8 PTH fragments (PTH28–84, 34–77, 34–84, 37–77, 37–84, 38–77, 38–84, and 45–84) were unequivocally identified and were shown to increase significantly when an eGFR declined to 17–23 mL/min/1.73m^2. Serum concentrations of PTH1–84 were similar when measured by LC-HRMS following capture by amino-terminal or carboxyl-terminal immunocapture methods. In patients with an eGFR of <30 mL/min/1.73 m^2, serum PTH concentrations measured using LC-HRMS were significantly lower than PTH measured using an iPTH immunoassay. PTH7–84 and oxidized forms of PTH1–84 were below the limit of detection (30 and 50 pg/mL, respectively).

CONCLUSIONS: LC-HRMS identifies circulating PTH1–84, carboxyl-terminal PTH fragments, and mid-region PTH fragments, in patients with progressive renal failure. Serum PTH1–84 and its fragments markedly rise when an eGFR decreases to 17–23 mL/min/1.73 m^2. PTH concentrations measured using LC-HRMS tend to be lower than those measured using an iPTH immunoassay, particularly in severe chronic renal failure. Our data do not support the existence of circulating PTH7–84 and oxidized PTH1–84.

Introduction

Parathyroid hormone (PTH) is synthesized in parathyroid glands (PTGs) as preproPTH, which is cleaved within the endoplasmic reticulum to yield proPTH, which is further processed in the Golgi complex to yield bioactive full-length PTH1–84 (1). Following secretion, circulating PTH1–84 is cleared by Kupffer cells, by proteolysis into amino-terminal (N-terminal) and carboxyl-terminal (C-terminal) fragments (2, 3). N-terminal PTH fragments are degraded in situ, whereas C-terminal PTH fragments are released into the circulation and cleared by the kidneys (4–6). C-terminal PTH fragments are also secreted by PTGs (7, 8). Plasma PTH fragment concentrations rise in chronic kidney disease (CKD) due to increased PTG function and impaired renal clearance (9).

Intact PTH (iPTH) immunoassays yield variable results in CKD, making it difficult to assess true PTH1–84 concentrations (10–17). To overcome difficulties associated with measurement of PTH1–84, and to define the nature and concentrations of PTH fragments in patients with CKD over a broad range of estimated glomerular filtration rates (eGFR), we developed a liquid chromatography-high resolution mass spectrometry (LC-HRMS) method that identified and quantified PTH1–84 and PTH fragments (18). While previous MS studies have measured PTH1–84 and PTH fragments in small patient numbers, no studies have

determined PTH1–84 and PTH fragment concentrations using MS with isotope-labeled internal standards (IS) in patients with varying eGFR (19–21). Knowledge of concentrations of PTH1–84 and its fragments is clinically relevant because serum iPTH concentrations in CKD are poorly correlated with the severity of renal osteodystrophy and fracture incidence. Moreover, PTH effects on bones are believed to be blocked by circulating PTH7–84 (22, 23).

Materials and Methods

STUDY COHORT

The Mayo Clinic Institutional Review Board approved the study. Residual waste serum samples were obtained from the routine clinical laboratory tests at the Central Clinical Laboratory from July through November 2019. The study was determined to be exempt from the requirement for the informed consent in accordance with applicable HIPAA regulations (45 CFR 46.116d, category 1). Non-identified information was used in order to protect the patient data confidentiality. For specimen collection, 5 mL of blood was collected into a serum-separating tube (SST), centrifuged for 5–10 min at 3200 rpm, and stored at 4 °C before analysis on the Roche Cobas iPTH immunoassay. Immediately after analysis, a 1.5–3.0 mL serum aliquot was removed from the SST and pipetted into a 13×75 mm polypropylene tube, and stored at −80 °C for the LC-HRMS method. Serum samples were analyzed within 3 months of collection, undergoing a single freeze/thaw cycle. Patients with a kidney transplant, primary hyperparathyroidism, recombinant PTH1–34 therapy, or biotin supplementation were excluded. The Chronic Kidney Disease Epidemiology Collaboration creatinine equation was used to classify CKD severity (CKD1: eGFR 90; CKD2: eGFR 60–89; CKD3a: eGFR 45–59; CKD3b: eGFR 30–44; CKD4: eGFR 15–29; and CKD5: eGFR <15 mL/min/1.73 m^2).

REAGENTS

Recombinant PTH1–84 (95/646) was from the National Institute for Biological Standards and Control (NIBSC; Hertfordshire, UK). Synthetic PTH peptides (PTH28–84, 34–77, 34–84, 37–77, 37–84, 38–77, 38–84, 45–84) and respective stable isotope-labeled IS ($^{13}C/^{15}N$-PTH28–84, $^{13}C/^{15}N$-PTH34–77, $^{13}C/^{15}N$-PTH34–84, $^{13}C/^{15}N$-PTH37–77, $^{13}C/^{15}N$-PTH37–84, $^{13}C/^{15}N$-PTH38–77, $^{13}C/^{15}N$-PTH38–84, and $^{13}C/^{15}N$-PTH45–84) were synthesized by Innovagen. U-^{15}N-PTH1–84, PTH7–84, and U-^{15}N-PTH7–84 were synthesized by GoldBio (online Supplemental Table 1). DDC Mass Spect Gold® serum (MSG®, vitamin D-free, human delipidized) was obtained from Golden West Biologicals. Synthetic peptide standards were prepared gravimetrically and stored in low protein binding Eppendorf tubes in 33% acetonitrile, 0.4% trifluoroacetic acid (TFA), and 0.05% bovine serum albumin (BSA) in water. Neat solutions of each unlabeled and stable-isotope labeled PTH peptide were analyzed by HPLC-UV for purity and by UHPLC-HRMS at each charge state for the presence of interfering species. Amino acid analysis was performed on powdered standards to determine the net peptide content. The stock concentrations were corrected based on purity of the solutions. Stock solutions (0.012–0.061 mg/mL for recombinant PTH1–84 and synthetic PTH peptides, and 0.019–0.057 mg/mL for IS) were prepared separately in 33% acetonitrile with 0.4% TFA and 0.05% BSA in water. Two

intermediate concentrations of calibrator and 7 working calibrator solutions were prepared in MSG® serum, with final dilutions generating a calibration curve containing 0–10000 pg/mL of each PTH peptide. Stock IS solutions of labeled PTH peptides were added to MSG® serum to achieve a working IS concentration of 19–42 ng/mL for each PTH peptide. Three ranges of concentrations (40–150, 150–500, and 500–2000 pg/mL) of quality control material were created by spiking calibration standard material into pooled human serum (SeraCare). Working solutions in MSG® serum and neat solutions (stocks and intermediate calibrators) were stable for 6 and 12 months, respectively, covering the duration of this study.

IMMUNOCAPTURE

Two immunocapture methods were developed. The C-terminal immunocapture method has been previously described (24). Briefly, polystyrene beads coated with affinity purified murine monoclonal anti-PTH (44–84) antibody (Immulite™ 2000 iPTH assay; Siemens) were placed into wells of a 96-well Isolute PPT+ filter plate (Biotage; one bead/well). Calibrators, quality controls, and patient serum samples were thawed, vortexed, and placed on ice prior to pipetting 1 mL of each into the plate. Fifty microliters of working IS mixture was added to each well. The plate was sealed, vortexed, and shaken at 20 °C for 4 h at 2500 rpm. After incubation, serum was discarded using a positive pressure manifold (Chrom Tech) and beads were washed first with 1.8 mL and then with 1.0 mL of 1X phosphate buffered saline. C-terminal PTH peptides bound to the antibody-bead were eluted with 330 μL of 1% formic acid into 96-well plates and stored at 4 °C until analysis.

For the N-terminal immunocapture method, 200 μL of calibrator, quality control or patient serum sample and 50 μL of IS were combined with 200 μL of biotinylated monoclonal anti-PTH (26–32) (antibody (2.3 mg/L) in a 96-well plate. The plate was sealed, vortexed and placed on an orbital plate shaker at 20 °C for 90 min. After incubation, 200 μL of streptavidin magnetic beads (0.72 mg/mL; Roche iPTH reagent) were added to each well and the plate was incubated on a plate shaker for 90 min. The plate was placed on a magnetic separator (Epigentek) and supernatant serum was aspirated. Beads were washed twice with 200 μL of 1X phosphate buffered saline and N-terminal PTH peptides bound to antibody were eluted with 330 μL of 1% formic acid, transferred into a 96-well plate, and stored at 4 °C until analysis.

LIQUID CHROMATOGRAPHY-HIGH RESOLUTION MASS SPECTROMETRY

PTH peptides in serum samples were measured using a Thermo UltiMate 3000 UHPLC system coupled to a Thermo Q Exactive Plus HRAM hybrid quadrupoleorbitrap mass spectrometer with a heated electrospray ionization source. Full MS centroided data were acquired in positive ion mode over mass-to-charge ratio (m/z), 303–800 m/z, with a 70 000 resolution relative to m/z 200 (Supplemental Table 2). To separate PTH1–84 and PTH fragments, reversed-phase chromatography was performed with a ProSwift RP-4H, monolithic HPLC column (1 × 250 mm) coupled to a 4 × 2.0 mm, C18 guard cartridge (Phenomenex). Mobile Phase (MP) A comprised 5% dimethylsulfoxide (DMSO) and 0.4% formic acid in water. MP B comprised 5% DMSO and 0.4% formic acid in acetonitrile. DMSO was utilized as a supercharging agent. Injection volume was 100 μL at a starting flow

rate of 150 μL/min, 100% MP A. This flow was held for 2 min after injection. MP B was increased to 50% over 15 min. The flow rate was increased to 320 μL/min over 1.5 min and was kept constant for 4.5 mins while MP B increased to 95% to wash the column. At 25-min, solvent was switched to 100% MP A and the flow rate was decreased to 150 μL/min over 3 min.

Retention time and optimal charge states of each PTH peptide were established by single peptide injections using 1.2–5.0 ng/mL solutions. Two or more charge states were monitored for each PTH peptide with a single charge state selected for quantitation based on intensity, reproducibility, and limited interference observed in serum samples (Supplemental Table 3). The same charge states were monitored for the unlabeled and labeled forms of the PTH peptide. Final monitored charge states for quantification were as follows: PTH1–84 at z= +15, PTH28–84 at z=+11, PTH34–77 at z=+8, PTH34–84 at z=+9, PTH37–77 at z=+7, PTH37–84 at z=+10, PTH38–77 at z=+7, PTH38–84 at z=+9, and PTH45–84 at z=+8. For serum oxidized PTH1–84, we acquired theoretical mass isotopic distribution profiles of 2 singly-oxidized and doubly-oxidized forms of PTH1–84: PTH1–84M8(O) +14, +15, +16; PTH1–84M18(O) +14, +15, +16; and PTH1–84M8(O)18(O) +14, +15, +16 (Supplemental Fig. 1).

Mass spectra were analyzed using the Thermo Xcalibur Qual Browser, v4.2. Sample analysis and quantification were performed using TraceFinder Clinical, v4.1. Theoretical masses of each PTH peptide and charge state were calculated using Molecular Weight Calculator, v6.50 and confirmed by injection of respective calibration standards. Quantitation was performed using a calibration curve with analyte-to-IS peak area ratios for each PTH peptide charge state with linear regression analysis and 1/X weighting. The 10 mostabundant isotopic masses for each charge state (for both PTH peptides and IS) were summed for quantitation. The mass tolerance was set to 10 ppm. IS recovery and retention time were monitored for PTH peptides

ANALYTICAL VALIDATION OF LC-HRMS

The criteria for assay acceptance included 7-point calibration curves with an R^2 >0.995 and no individual point exceeding ±20% of the expected value for PTH peptides. The limit of detection (LOD) was defined as a signal-to-noise ratio 3 in the lowest-concentration calibrators (ranging from 24 to 81 pg/mL), and the lower limit of quantification (LLOQ) was calculated from inter-assay imprecision of quality control material (Supplemental Figs. 2 and 3; Supplemental Table 4). The LLOQ for all PTH peptides was achieved by summing of 10 isotopic ions within each charge envelope combined with the supercharging effects of DMSO in the MP, which reduced the charge states from ~10 to ~3 (Supplemental Fig. 4). For chromatographic peaks lacking Gaussian distribution, spectral data and isotopic envelopes were reviewed. Retention time acceptance criteria and IS peak area flagging were used as qualitative criteria for the acceptability assessment. Quality control materials consisting of pooled human serum spiked with PTH peptides were used for imprecision studies. Intra-assay imprecision was determined by assaying 12 replicates of each of 3 quality control samples within 1 assay, and inter-assay imprecision was calculated from 10 replicates of each of 3 quality control samples across 5 batches. Imprecision was expressed

as the percentage coefficient of variation (%CV). Recovery was determined by spiking 100, 500, and 1000 pg/mL of each synthetic PTH peptide into 4 patient serum matrices of varying PTH concentrations. Expected values were determined by summing the spiked concentration with the endogenous concentration. Percent recovery was determined as (Measured/ Expected concentration) x100.

ROCHE IPTH IMMUNOASSAY

Serum iPTH concentrations were measured using an iPTH electrochemiluminescence immunoassay and a Roche Cobas e411 analyzer. A biotinylated monoclonal antibody reacts with the N-terminus (amino acids 26–32) and a ruthenium-labeled monoclonal antibody reacts with the C-terminus (amino acids 37–42) of PTH. The method has a %CV of <20% and LLOQ of 6 pg/mL.

To determine if PTH fragments cross-react with an iPTH immunoassay, synthetic PTH fragments (PTH7–84, 28–84, 34–84, 35–84, 37–84, 38–84, 45–84, 48–84) were spiked individually and in combination at concentrations between 30 and 3000 pg/mL in vitamin D-depleted serum prior to measurement.

DETERMINATION OF STABILITY OF PTH AND PTH FRAGMENTS

The stability of PTH1–84 and PTH fragments in freshly-collected serum samples and serum samples stored at −80 °C was assessed in patients with eGFRs >60 and <30 mL/min/1.73 m^2. Serum concentrations of Roche iPTH, LC-HRMS PTH1–84, and PTH fragments were measured at baseline and 1-week apart. To show that PTH fragments were not generated in vitro, vitamin D-depleted serum, human stripped serum, and patient serum samples were spiked with PTH1–84 or PTH7–84 to induce forced degradation at room temperature. The effect of freeze-thaw cycles on PTH1–84 and PTH fragment stability was evaluated in patient serum samples.

STATISTICAL ANALYSES

Continuous variables were compared using one-way ANOVA or the Kruskal-Wallis test with Bonferroni correction for multiple comparisons. For non-normally distributed variables, median with interquartile ranges (IQ25 and IQ75) are presented. Categorical variables were compared using the chi-square test. We examined interrelationships of analytes using Pearson's correlation coefficients. A segmented regression model was used to detect thresholds at which a statistically significant change was observed in the slope of serum analyte concentrations in relation to eGFR (25). PTH concentrations measured by LC-HRMS and iPTH immunoassay were compared using Bland-Altman analysis. Analyses were performed using Stata version 14.0. P values <0.05 were considered statistically significant.

Results

A total of 221 patients with varying eGFR were included in the study. The mean age of subjects was 61.4 ± 14.8 years and 43% were men. Serum phosphate concentrations remained unchanged across CKD1–3 stages, and then increased progressively in patients

with CKD4–5. Serum iPTH and intact fibroblast growth factor 23 (iFGF23) concentrations increased modestly in patients with CKD1–3. Only patients with CKD4–5 demonstrated statistically significant increases in serum iPTH and iFGF23 concentrations relative to patients with CKD1–2 (Table 1).

PERFORMANCE CHARACTERISTICS OF LC-HRMS

Calibrators and quality control materials containing PTH1–84 and synthetic PTH fragments were analyzed by N-terminal and C-terminal immunocapture methods. We detected PTH1–84 by LC-HRMS in similar concentrations following N-terminal and C-terminal immunocapture (Fig. 1). The LOD for PTH1–84 with both immunocapture methods was 50 pg/mL. Calibration curves were linear and reproducible (R^2 >0.995) for both methods. Mean intra-assay and inter-assay %CVs were 17% and 19% for PTH1–84, and were 18% and 23% for other PTH peptides, respectively. Mean percent recovery of PTH peptides in human pooled serum was 107% (range 88% to 126%). Peak shape was shown to be reproducible over time and retention time changes were minimal between lots of MPs and analytical columns. Carryover, monitored by performing a blank injection after the highest calibrator was acceptable, defined as less than the LOD for each PTH peptide.

SPECIES OF HUMAN PTH FRAGMENTS DETERMINED BY LC-HRMS

We detected 8 species of PTH fragments in human serum: PTH28–84, 34–77, 34–84, 37–77, 37–84, 38–77, 38–84, and 45–84 (Fig. 2; Supplemental Figs. 5 and 6). No N-terminal PTH fragments (e.g., PTH1–34) were detected using the N-terminal immunocapture method. The LOD of the C-terminal immunocapture method for circulating PTH fragments ranged from 24 to 81 pg/mL. Serum PTH7–84 was below the LOD (30 pg/mL) using both immunocapture methods (Supplemental Fig. 7). Synthetic PTH1–34 and PTH7–34 added to serum matrix were readily detected with the N-terminal immunocapture method. While synthetic PTH35–84 was captured using the C-terminal immunocapture method, $^{13}C^{15}$N-PTH35–84 was unstable and therefore quantitative data were not obtained. Synthetic PTH48–84 had poor analytical sensitivity using the C-terminal immunocapture method, and appropriate calibration could not be generated (R^2 <0.995).

Serum concentrations of PTH1–84 and PTH fragments increased as eGFR declined (Table 2), and increased significantly when an eGFR decreased to 17–23 mL/min/1.73 m^2 (Fig. 3, Supplemental Table 5). The greatest change in circulating PTH fragment concentrations with decreasing eGFR was observed with PTH38–77. Serum concentrations of PTH fragments increased in parallel as PTH1–84 increased (Supplemental Fig. 8, Supplemental Table 6). There were weak or no associations between serum PTH fragments and serum phosphate concentrations (Supplemental Fig. 9).

STABILITY OF PTH AND PTH FRAGMENTS

Mean changes of serum concentrations of Roche iPTH, LC-HRMS PTH1–84, and PTH37–84 after 1-week storage at −80 °C (n = 4) were −2.7% (95% CI, −7.15% to 5.68%; *P*=0.78), +14% (95% CI, −19.56% to 20.92%; *P*=0.46), −9% (95% CI, −14.68% to 6.69%; *P*=0.65), respectively. Characterized PTH fragments were not generated in vitro in vitamin D-depleted serum, human stripped serum, and freshly collected serum from patients with high

or low eGFRs spiked with PTH1–84 and PTH7–84 and stored at room temperature for 6 or 16 h (Supplemental Figs. 10 and 11). Spiked serum concentrations of LC-HRMS PTH1–84 and PTH fragments changed −25 to +24% after 1 freeze-thaw cycle, and changed −45% to +24% after 2 freeze-thaw cycle (Supplemental Table 7). In the spike-and-recovery experiment (n = 4 per group), percent recovery of LC-HRMS PTH1–84 between high- and low-eGFR patient serum samples were 84% and 86%, respectively, (mean difference of 2.23%; 95% CI, −8.74% to 13.12%; *P* = 0.63).

DETERMINATION OF OXIDIZED PTH1–84 BY LC-HRMS

Singly-oxidized or doubly-oxidized forms of PTH1–84 [PTH1–84M8(O) +14, +15, +16; PTH1–84M18(O) +14, +15, +16; and PTH1–84M8(O)18(O) +14, +15, +16] were undetectable in patient serum samples with high or low eGFR and with PTH1–84 concentrations of <1000 pg/mL.

METHOD COMPARISON

Significant correlations between serum PTH concentrations measured using the Roche iPTH immunoassay and LC-HRMS method were observed in patients with CKD3–5 (Fig. 4). Bland-Altman analysis demonstrated that serum PTH measured using LC-HRMS were 58% lower than those determined by an iPTH immunoassay (95% CI: −150% to 35%). The negative bias for the LC-HRMS method compared with an iPTH immunoassay in patients with CKD3, CKD4, and CKD5 was −13% (95% CI: −93% to 68%), −74% (95% CI: −135% to −13%), and −86% (95% CI: −132% to −40%), respectively (Supplemental Fig. 12).

Serum iPTH concentrations increased modestly in patients with CKD1–3 and then increased significantly in CKD4–5, whereas serum LC-HRMS PTH1–84 concentrations increased significantly only in patients with CKD5 versus CKD1–2 (*P* = 0.02). In patients with CKD4–5, serum concentrations of PTH measured using LC-HRMS method were significantly lower than those measured using an iPTH immunoassay (Supplemental Fig. 13).

Cross-Reactivity of PTH Fragments with Roche iPTH Immunoassay—Synthetic PTH fragments (PTH28–84, 34–84, 35–84, 37–84, 38–84, 45–84, 48–84), tested individually and in combination, showed negligible cross-reactivity with an iPTH immunoassay. Conversely, an iPTH immunoassay detected synthetic PTH7–84 at close to 100% cross-reactivity (Supplemental Table 8).

Discussion

We identified and quantitated serum full-length PTH1–84 and PTH fragments (PTH28–84, 34–77, 34–84, 37–77, 37–84, 38–77, 38–84, 45–84) using LC-HRMS in patients with varying eGFR values. Serum PTH7–84 and oxidized forms of PTH were not detected. We show here that serum concentrations of PTH fragments rise significantly when an eGFR falls to 17–23 mL/min/1.73 m^2. In patients with an eGFR of <30 mL/min/1.73 m^2, serum PTH concentrations measured using LC-HRMS are significantly lower than those measured using an iPTH immunoassay.

While some studies have identified PTH7–84 as an abundant circulating PTH fragment (16, 26), others have shown that PTH7–84 is undetectable using MS in human plasma (19–21). The latter results are consistent with our findings of PTH7–84 concentrations below the LOD (30 pg/mL). Thus, PTH7–84 may not be present in concentrations sufficient to alter bioactivity of PTH1–84 in vivo (19–21). These findings are important because of the antagonistic effects of synthetic PTH7–84 on PTH1–84 bioactivity in bones and kidneys (22, 27, 28).

In a previous study (19), circulating PTH fragments were measured using matrix-assisted laser desorption/ionization-time of flight (MALDI-TOF) MS; 4 PTH fragments (PTH34–84, 37–84, 38–84, 45–84) were identified in 4 CKD patients, and in 6 healthy women given PTH1–84 parenterally. A subsequent study using post-immunocapture trypsin digestion followed by MALDI-TOF MS found similar PTH fragments plus five additional PTH fragments (PTH28–84, 34–77, 37–77, 38–77, 48–84) from the plasma of 12 healthy and 12 CKD5 patients (21).

Our LC-HRMS method offers advantages over previously published MS methods (Supplemental Table 9). By including analytical standards and stable isotope-labeled IS, we definitively quantify serum PTH1–84 and PTH fragments. Intact protein analysis using LC-HRMS allows specific detection of all captured PTH peptides while maintaining analytical sensitivity (29). Assays using enzymatic digestion are difficult to optimize, and rely on unique tryptic peptides that must ionize efficiently and be traceable back to each specific PTH peptide (18, 30). An additional advantage of operating in full scan mode is the ability to detect circulating PTH fragments for which analytical standards are unavailable. Furthermore, the addition of 5% DMSO to solvents during ionization of peptides facilitates enhanced ionization efficiency and coalescence of ion current into fewer charge states, resulting in higher quality spectra and greater analytical sensitivity.

We confirmed the absence of circulating N-terminal PTH fragments, and the presence of C-terminal and mid-region PTH fragments. The generation of C-terminal PTH fragments in the PTGs is associated with endopeptidase activity in the Golgi complex (31), whereas lysosomal cathepsin D activity produces C-terminal PTH fragments in Kupffer cells (32). Some mid-region PTH fragments detected (PTH34–77, 37–77, 38–77) could be generated by C-terminal proteolytic cleavage of longer PTH fragments (33). Previous studies in which PTH fragments with N-termini at amino acid 24, 35, 41 and 43 were identified, were performed in animal models using radioactive-labeled PTH (6, 31, 32, 34).

We showed that no statistical difference was observed for the eGFR thresholds at which serum Roche iPTH and LC-HRMS PTH1–84 increased. The low prevalence of hyperphosphatemia in our cohort might result in the development of a lesser iPTH increase at a lower eGFR compared with previous studies (35, 36). We observed a significant increase in circulating PTH fragment concentrations when eGFR decreased to 17–23 mL/min/1.73 m^2. The potential mechanisms underlying this phenomenon are the decreased renal clearance and increased secretion of PTH fragments from the hyperplastic PTGs. The kidneys remove circulating C-terminal PTH fragments by glomerular filtration and fragments are subsequently metabolized in renal tubular cells; therefore, a reduction in

eGFR contributes to the increase in circulating PTH fragments (4–6, 37). However, PTH1–84 is rapidly transported through the basolateral membrane and is then degraded within proximal tubular cells; hence, a decrease in eGFR might have less impact on circulating PTH1–84 concentration (38).

Differences in serum iPTH concentrations are noted with various iPTH immunoassays. A study comparing the serum iPTH measured with 13 iPTH immunoassays in CKD5 patients, found that a median bias of 44.9% to 123.0% existed between a given iPTH immunoassay and the reference Allegro iPTH immunoassay (10). Our study confirms inter-assay discrepancies in iPTH results, and highlights the need for more accurate methods for the PTH measurement (11, 12).

Serum LC-HRMS PTH1–84 concentrations were approximately 13% lower in CKD3 and 74% to 86% lower in CKD4–5 compared with Roche iPTH concentrations. Several factors might account for these differences. First, some PTH fragments undetected by LC-HRMS may cross-react with iPTH immunoassays. Second, partial degradation of PTH could occur during sample storage. PTH remained stable at −80 °C for 1 week; however, we did not test stability for any longer period of time. Third, heterophile antibodies may cause interference with iPTH immunoassays (39). Fourth, uremic toxins in CKD may confer interference through the "matrix effects" (40). Notably, in this study, PTH standardization was attained using the same international standard (NIBSC 95/646) for both methods. Although oxidized PTH was claimed to cross-react with iPTH immunoassays (41), it was below the LOD (50 pg/mL) for PTH1–84 by our LC-HRMS.

The strengths of our study include the measurement of serum PTH1–84 and PTH fragments in patients with varying eGFRs and the use of LC-HRMS method specifically developed for the peptides of interest. Our study has certain limitations. First, the immunocapture method could potentially fail to capture some PTH fragments. The LLOQ for PTH peptides is limited but it could be optimized with increased serum volume and improvements in chromatographic techniques. Lastly, we lack data on the correlations between serum concentrations of PTH1–84, including PTH fragments, and bone histomorphometry. Further studies are also needed to assess the accuracy of LC-HRMS method.

Conclusions

LC-HRMS identifies circulating PTH1–84, C-terminal PTH fragments, and mid-region PTH fragments in patients with renal dysfunction. Serum PTH1–84 and its fragments increase as eGFR declines. PTH concentrations measured using LC-HRMS tend to be lower than those measured using an iPTH immunoassay, particularly in advanced CKD. Our data do not support the existence of circulating PTH7–84 and oxidized PTH1–84.

Supplementary Material

Refer to Web version on PubMed Central for supplementary material.

Role of Sponsor:

The funding organizations played a direct role in the design of study, choice of enrolled patients, review and interpretation of data, preparation of manuscript, and final approval of manuscript.

Nonstandard Abbreviations:

PTH	parathyroid hormone
PTGs	parathyroid glands
N-terminal	amino-terminal
C-terminal	carboxyl-terminal
CKD	chronic kidney disease
iPTH	intact PTH
eGFR	estimated glomerular filtration rate
LC-HRMS	liquid chromatography-high resolution mass spectrometry
IS	internal standard
SST	serum-separating tube
NIBSC	National Institute for Biological Standards and Control
MSG	Mass Spect Gold®
TFA	trifluoroacetic acid
BSA	bovine serum albumin
UHPLC	ultra-high-performance liquid chromatography
rpm	revolutions per minute
m/z	mass-to-charge ratio
MP	mobile phase
DMSO	dimethyl sulfoxide
LOD	limit of detection
LLOQ	lower limit of quantitation
CV	coefficient of variation
IQR	interquartile range
iFGF23	intact fibroblast growth factor 23
MALDI-TOF	matrix-assisted laser desorption/ionization-time of flight

REFERENCES

1. Habener JF, Amherdt M, Ravazzola M, Orci L. Parathyroid hormone biosynthesis. Correlation of conversion of biosynthetic precursors with intracellular protein migration as determined by electron microscope autoradiography. J Cell Biol 1979;80:715–31. [PubMed: 457765]

2. D'Amour P, Huet PM, Segre GV, Rosenblatt M. Characteristics of bovine parathyroid hormone extraction by dog liver in vivo. Am J Physiol 1981;241: E208–214. [PubMed: 7025656]

3. Rouleau MF, Warshawsky H, Goltzman D. Parathyroid hormone binding in vivo to renal, hepatic, and skeletal tissues of the rat using a radioautographic approach. Endocrinology 1986;118:919–31. [PubMed: 3948781]

4. Martin K, Hruska K, Greenwalt A, Klahr S, Slatopolsky E. Selective uptake of intact parathyroid hormone by the liver: differences between hepatic and renal uptake. J Clin Invest 1976;58:781–8. [PubMed: 965485]

5. Bringhurst FR, Stern AM, Yotts M, Mizrahi N, Segre GV, Potts JT. Peripheral metabolism of [35S]parathyroid hormone in vivo: influence of alterations in calcium availability and parathyroid status. J Endocrinol 1989;122: 237–45. [PubMed: 2769152]

6. Bringhurst FR, Stern AM, Yotts M, Mizrahi N, Segre GV, Potts JT. Peripheral metabolism of PTH: fate of biologically active amino terminus in vivo. Am J Physiol 1988; 255:E886–893. [PubMed: 3202165]

7. D'Amour P, Räkel A, Brossard J-H, Rousseau L, Albert C, Cantor T. Acute regulation of circulating parathyroid hormone (PTH) molecular forms by calcium: utility of PTH fragments/PTH(1–84) ratios derived from three generations of PTH assays. J Clin Endocrinol Metab 2006;91: 283–9. [PubMed: 16219713]

8. D'Amour P, Palardy J, Bahsali G, Mallette LE, DeLéan A, Lepage R. The modulation of circulating parathyroid hormone immunoheterogeneity in man by ionized calcium concentration. J Clin Endocrinol Metab 1992;74: 525–32. [PubMed: 1740486]

9. Patel S, Barron JL, Mirzazedeh M, Gallagher H, Hyer S, Cantor T, Fraser WD. Changes in bone mineral parameters, vitamin D metabolites, and PTH measurements with varying chronic kidney disease stages. J Bone Miner Metab 2011;29:71–9. [PubMed: 20521154]

10. Souberbielle J-C, Boutten A, Carlier M-C, Chevenne D, Coumaros G, Lawson-Body E, et al. Inter-method variability in PTH measurement: implication for the care of CKD patients. Kidney Int 2006;70:345–50. [PubMed: 16788691]

11. Eddington H, Hudson JE, Oliver RL, Fraser WD, Hutchison AJ, Kalra PA. Variability in parathyroid hormone assays confounds clinical practice in chronic kidney disease patients. Ann Clin Biochem 2014;51: 228–36. [PubMed: 24000371]

12. Joly D, Drueke TB, Alberti C, Houillier P, Lawson-Body E, Martin KJ, et al. Variation in serum and plasma PTH levels in second-generation assays in hemodialysis patients: a cross-sectional study. Am J Kidney Dis 2008; 51:987–95. [PubMed: 18430500]

13. Blind E, Schmidt-Gayk H, Scharla S, Flentje D, Fischer S, Göhring U, et al. Two-site assay of intact parathyroid hormone in the investigation of primary hyperparathyroidism and other disorders of calcium metabolism compared with a midregion assay. J Clin Endocrinol Metab 1988;67:353–60. [PubMed: 3292561]

14. Endres DB, Villanueva R, Sharp CF, Singer FR. Immunochemiluminometric and immunoradiometric determinations of intact and total immunoreactive parathyrin: performance in the differential diagnosis of hypercalcemia and hypoparathyroidism. Clin Chem 1991; 37:162–8. [PubMed: 1993319]

15. Michelangeli VP, Heyma P, Colman PG, Ebeling PR. Evaluation of a new, rapid and automated immunochemiluminometric assay for the measurement of serum intact parathyroid hormone. Ann Clin Biochem 1997;34: 97–103. [PubMed: 9022895]

16. Lepage R, Roy L, Brossard JH, Rousseau L, Dorais C, Lazure C, et al. A non-(1–84) circulating parathyroid hormone (PTH) fragment interferes significantly with intact PTH commercial assay measurements in uremic samples. Clin Chem 1998;44:805–9. [PubMed: 9554492]

17. John MR, Goodman WG, Gao P, Cantor TL, Salusky IB, Jüppner H. A novel immunoradiometric assay detects full-length human PTH but not amino-terminally truncated fragments: implications

for PTH measurements in renal failure. J Clin Endocrinol Metab 1999;84: 4287–90. [PubMed: 10566687]

18. Couchman L, Taylor DR, Krastins B, Lopez MF, Moniz CF. LC-MS candidate reference methods for the harmonisation of parathyroid hormone (PTH) measurement: a review of recent developments and future considerations. Clin Chem Lab Med 2014;52:1251–63. [PubMed: 24762644]

19. Zhang C-X, Weber BV, Thammavong J, Grover TA, Wells DS. Identification of carboxyl-terminal peptide fragments of parathyroid hormone in human plasma at low-picomolar levels by mass spectrometry. Anal Chem 2006;78:1636–43. [PubMed: 16503617]

20. Singh RJ, Hines JM, Lopez MF, Krastins B, Hoofnagle AN. Mass spectrometric immunoassay raises doubt for the existence of parathyroid hormone fragment 7–84. Clin Chem 2015;61:558–60. [PubMed: 25597752]

21. Lopez MF, Rezai T, Sarracino DA, Prakash A, Krastins B, Athanas M, et al. Selected reaction monitoring-mass spectrometric immunoassay responsive to parathyroid hormone and related variants. Clin Chem 2010;56: 281–90. [PubMed: 20022981]

22. Langub MC, Monier-Faugere M-C, Wang G, Williams JP, Koszewski NJ, Malluche HH. Administration of PTH-(7–84) antagonizes the effects of PTH-(1–84) on bone in rats with moderate renal failure. Endocrinology 2003;144: 1135–8. [PubMed: 12639892]

23. Huan J, Olgaard K, Nielsen LB, Lewin E. Parathyroid hormone 7–84 induces hypocalcemia and inhibits the parathyroid hormone 1–84 secretory response to hypocalcemia in rats with intact parathyroid glands. J Am Soc Nephrol 2006;17:1923–30. [PubMed: 16707565]

24. Kumar V, Barnidge DR, Chen L-S, Twentyman JM, Cradic KW, Grebe SK, et al. Quantification of serum 1–84 parathyroid hormone in patients with hyperparathyroidism by immunocapture in situ digestion liquid chromatography-tandem mass spectrometry. Clin Chem 2010;56:306–13. [PubMed: 20007860]

25. D'Amour P, Brossard J-H, Rousseau L, Nguyen-Yamamoto L, Nassif E, Lazure C, et al. Structure of non-(1–84) PTH fragments secreted by parathyroid glands in primary and secondary hyperparathyroidism. Kidney Int 2005;68:998–1007. [PubMed: 16105030]

26. Slatopolsky E, Finch J, Clay P, Martin D, Sicard G, Singer G, et al. A novel mechanism for skeletal resistance in uremia. Kidney Int 2000;58:753–61. [PubMed: 10916099]

27. D'Amour P Circulating PTH molecular forms: what we know and what we don't. Kidney Int Suppl 2006;102: S29–33.

28. Lesur A, Domon B. Advances in high-resolution accurate mass spectrometry application to targeted proteomics. Proteomics 2015;15:880–90. [PubMed: 25546610]

29. Neubert H, Shuford CM, Olah TV, Garofolo F, Schultz GA, Jones BR, et al. Protein biomarker quantification by immunoaffinity liquid chromatography-tandem mass spectrometry: current state and future vision. Clin Chem 2020;66:282–301. [PubMed: 32040572]

30. MacGregor RR, Jilka RL, Hamilton JW. Formation and secretion of fragments of parathormone. Identification of cleavage sites. J Biol Chem 1986;261:1929–34. [PubMed: 3944119]

31. Pillai S, Zull JE. Production of biologically active fragments of parathyroid hormone by isolated Kupffer cells. J Biol Chem 1986;261:14919–23. [PubMed: 3771558]

32. Pastor R, Guallar E. Use of two-segmented logistic regression to estimate change-points in epidemiologic studies. Am J Epidemiol 1998;148:631–42. [PubMed: 9778169]

33. Wu TL, Vasavada RC, Yang K, Massfelder T, Ganz M, Abbas SK, et al. Structural and physiologic characterization of the mid-region secretory species of parathyroid hormone-related protein. J Biol Chem 1996;271:24371–81. [PubMed: 8798692]

34. MacGregor RR, McGregor DH, Lee SH, Hamilton JW. Structural analysis of parathormone fragments elaborated by cells cultured from a hyperplastic human parathyroid gland. Bone Miner 1986;1:41–50. [PubMed: 3508716]

35. Muntner P, Jones TM, Hyre AD, Melamed ML, Alper A, Raggi P, et al. Association of serum intact parathyroid hormone with lower estimated glomerular filtration rate. Clin J Am Soc Nephrol 2009;4:186–94. [PubMed: 19019998]

36. Isakova T, Wahl P, Vargas GS, Gutiérrez OM, Scialla J, Xie H; on behalf of the Chronic Renal Insufficiency Cohort (CRIC) Study Group, et al. Fibroblast growth factor 23 is elevated before

parathyroid hormone and phosphate in chronic kidney disease. Kidney Int 2011;79:1370–8. [PubMed: 21389978]

37. Martin KJ, Hruska KA, Lewis J, Anderson C, Slatopolsky E. The renal handling of parathyroid hormone. Role of peritubular uptake and glomerular filtration. J Clin Invest 1977;60:808–14. [PubMed: 893678]

38. Yamashita H, Gao P, Cantor T, Futata T, Murakami T, Uchino S, et al. Large carboxy-terminal parathyroid hormone (PTH) fragment with a relatively longer half-life than 1–84 PTH is secreted directly from the parathyroid gland in humans. Eur J Endocrinol 2003;149:301–6. [PubMed: 14514344]

39. Levinson SS, Miller JJ. Towards a better understanding of heterophile (and the like) antibody interference with modern immunoassays. Clin Chim Acta 2002;325:1–15. [PubMed: 12367762]

40. Nicolò AD, Cantù M, D'Avolio A. Matrix effect management in liquid chromatography mass spectrometry: the internal standard normalized matrix effect. Bioanalysis 2017;9:1093–105. [PubMed: 28737421]

41. Hocher B, Armbruster FP, Stoeva S, Reichetzeder C, Grön HJ, Lieker I, et al. Measuring parathyroid hormone (PTH) in patients with oxidative stress–do we need a fourth generation parathyroid hormone assay? PloS One 2012;7:e40242. [PubMed: 22792251]
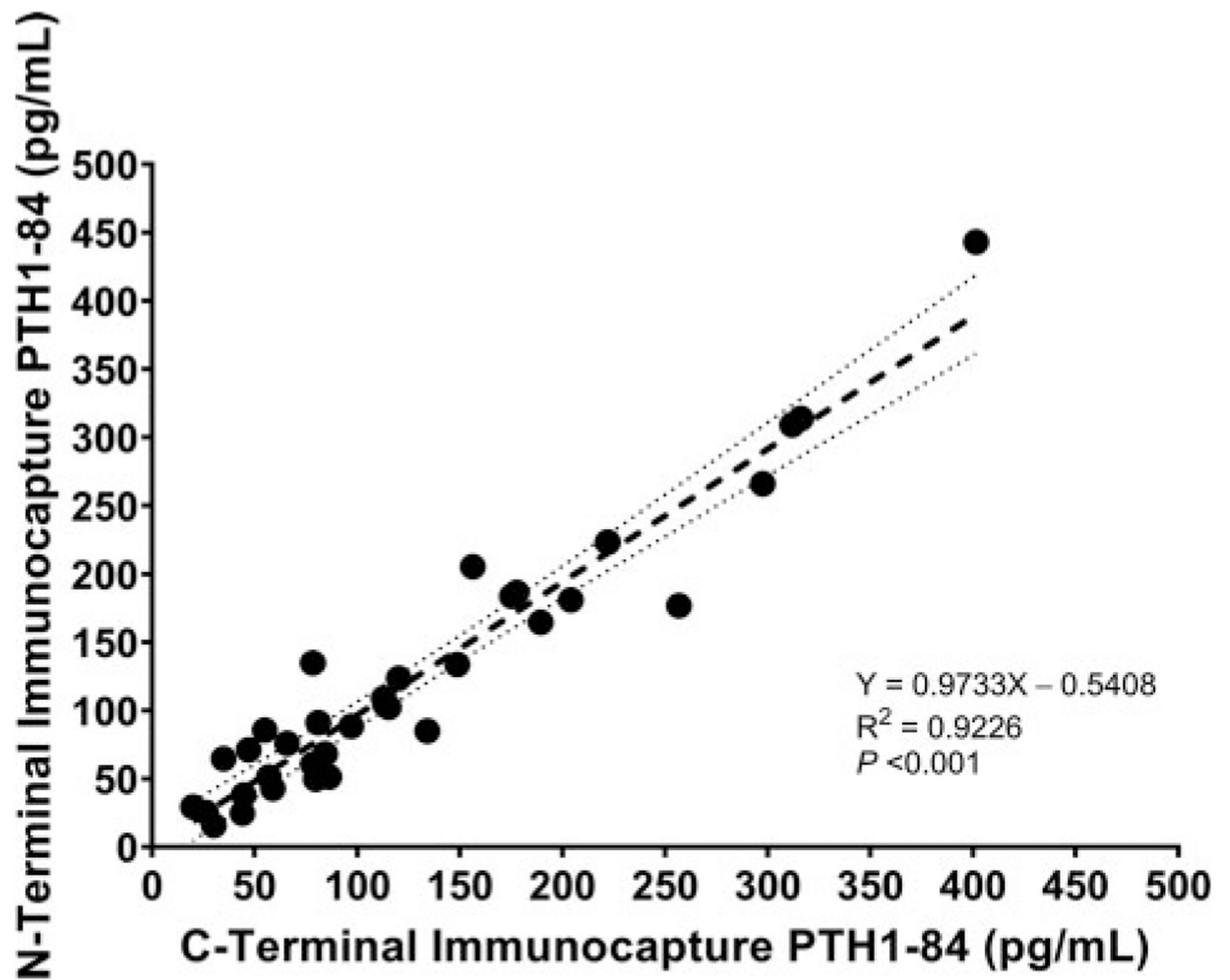
Fig. 1.
Correlation between serum concentrations of PTH1–84 measured using N-terminal and C-terminal immunocapture LC-HRMS methods. The shadowed area represents 95% confidence interval for the regression line.

Fig. 2.
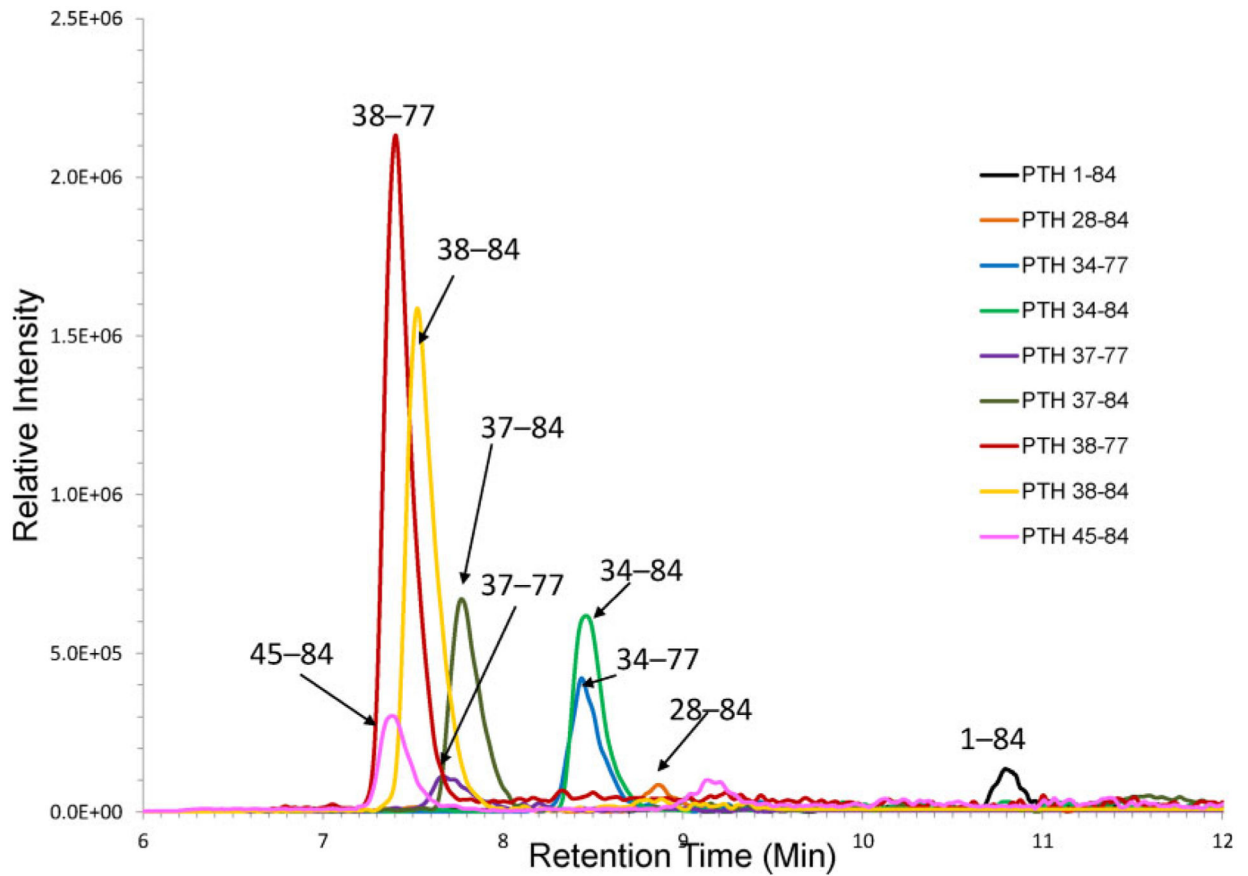Chromatogram depicting PTH1–84 and PTH fragments in a patient with stage 5 CKD. All peptides were determined by the C-terminal immunocapture LC-HRMS method and serum concentrations were as follows: PTH1–84 (204 pg/mL), PTH28–84 (193 pg/mL), PTH34–77 (225 pg/mL), PTH34–84 (1,043 pg/mL), PTH37–77 (551 pg/mL), PTH37–84 (799 pg/mL), PTH38–77 (1,716 pg/mL), PTH38–84 (396 pg/mL), PTH45–84 (414 pg/mL).
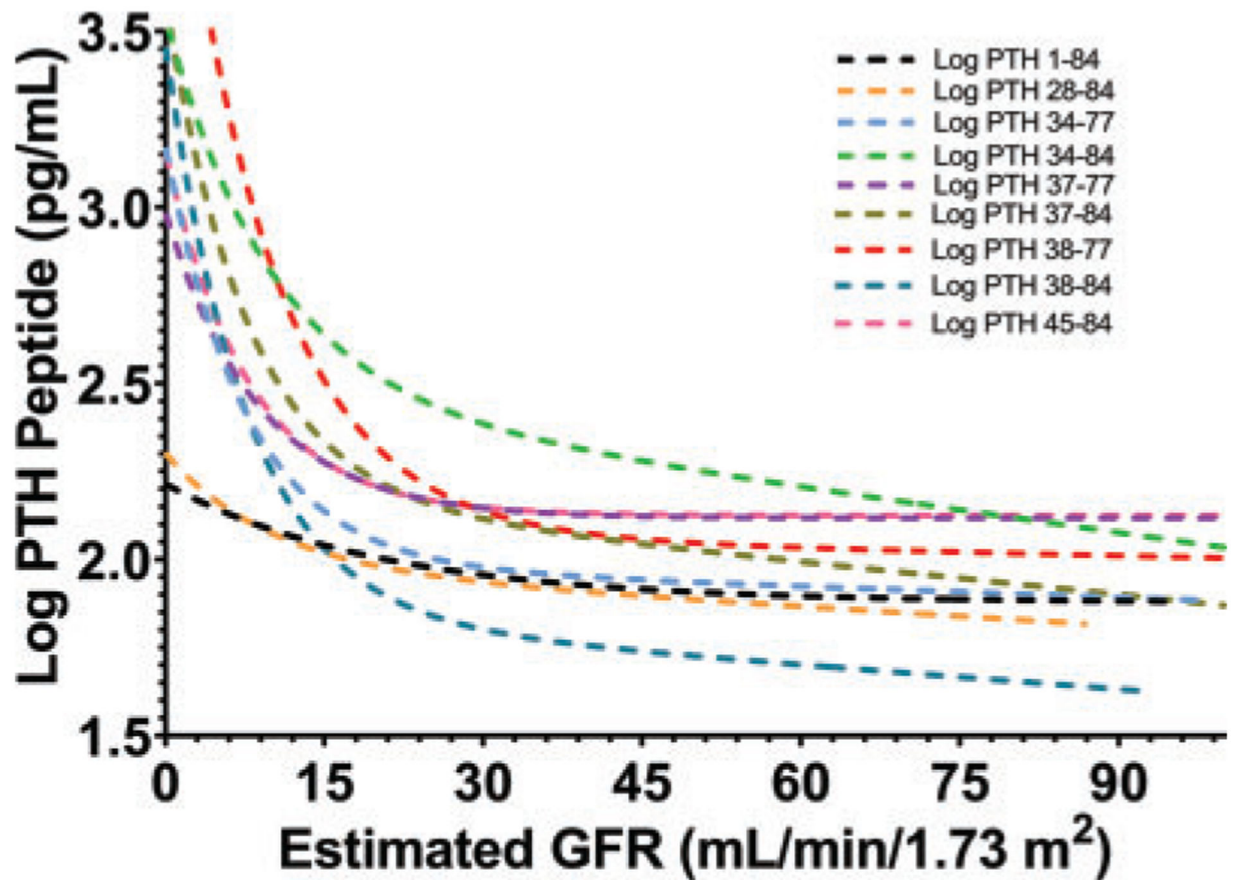
Fig. 3.
The associations of estimated GFR with log-transformed concentrations of PTH1–84 and PTH fragments: PTH1–84 ($y=2.0552e^{-0.002x}$; $R^2 = 0.42$; $P=0.039$), PTH28–84 ($y=2.0928e^{-0.002x}$; $R^2 = 0.31$; $P=0.004$), PTH34–77 ($y=2.3084e^{-0.003x}$; $R^2 = 0.36$; $P=0.005$), PTH34–84 ($y=2.7453e^{-0.004x}$; $R^2 = 0.41$; $P=0.016$), PTH37–77 ($y=2.35e^{-0.002x}$; $R^2 = 0.38$; $P=0.010$), PTH37–84 ($y=2.4876e^{-0.004x}$; $R^2 = 0.33$; $P=0.012$), PTH38–77 ($y=2.7707e^{-0.006x}$; $R^2 = 0.38$; $P=0.003$), PTH38–84 ($y=2.2597e^{-0.006x}$; $R^2 = 0.32$; $P=0.009$), PTH45–84 ($y=2.3842e^{-0.002x}$; $R^2 = 0.27$; $P=0.020$).

Fig. 4.
Correlations between LC-HRMS PTH1–84 and Roche iPTH results obtained in (A) CKD3–5, (B) CKD3, (C) CKD4, and (D) CKD5. The shadowed area represents 95% confidence interval for the regression line. CKD, chronic kidney disease.
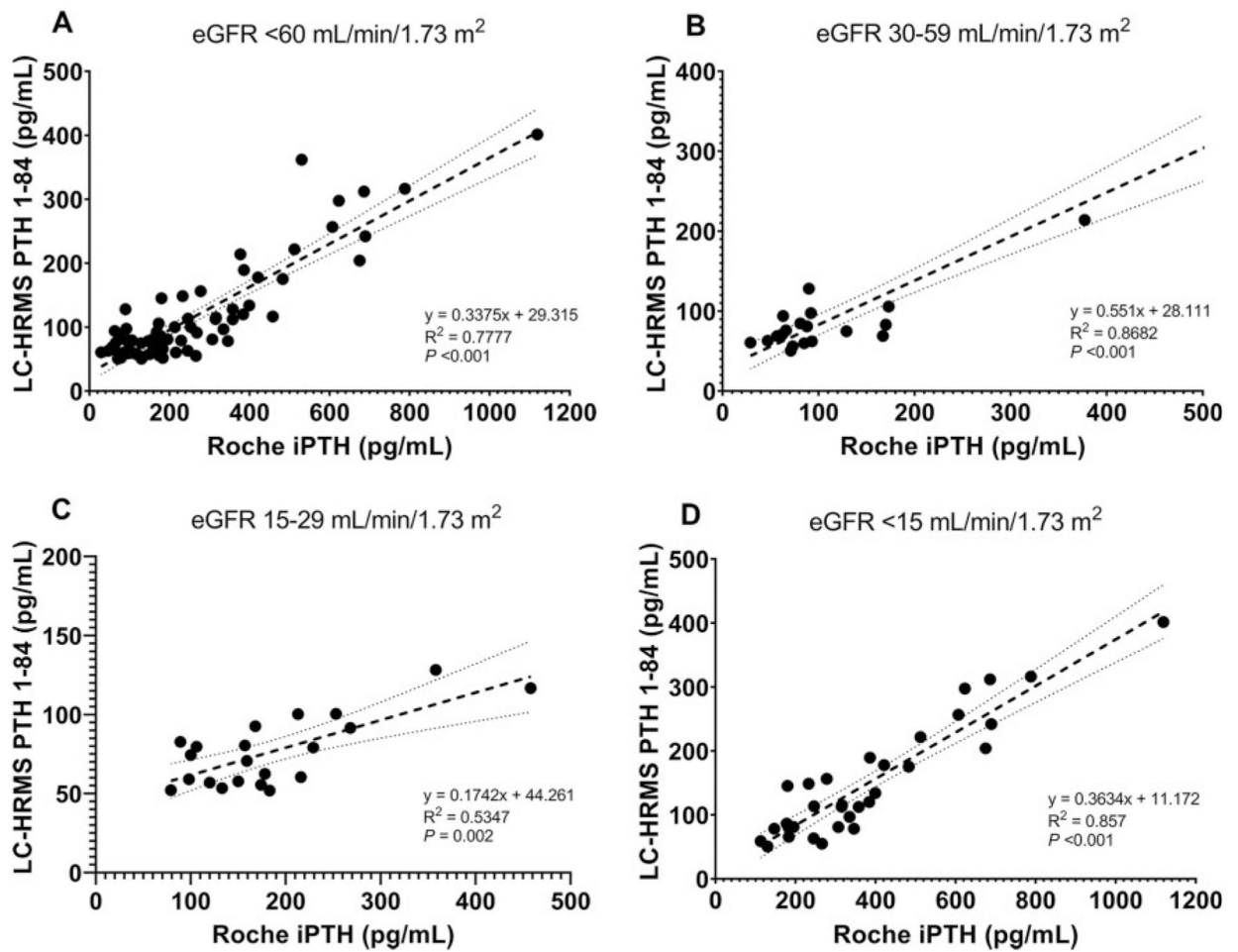
Table 1.

Clinical characteristics of the study patients according to stages of renal function.

Characteristics	Estimated GFR (mL/min/1.73 m²)					P for trend
	>60 (n = 60)	45–59 (n = 28)	30–44 (n = 32)	15–29 (n = 57)	<15 (n = 44)	
Age (years)	58.9±15.1	63.8±13.0	67.3±13.2	63.1±14.8	56.9±14.8	0.10
Female (no. [%])	44 (73.3)	17 (60.7)	17 (53.1)	30 (52.6)	17 (38.6)[i]	0.01
Diabetes (no. [%])	7 (11.7)	8 (28.6)	12 (37.5)	23 (40.4)[ii]	18 (40.9)[i]	0.006
Hypertension (no. [%])	30 (50)	19 (67.9)	27 (84.4)	48 (84.2)[i]	38 (86.4)[i]	0.009
History of fracture (no. [%])	1 (1.7)	2 (7.1)	2 (6.3)	2 (3.5)	1 (2.3)	0.64
Calcium use (no. [%])	18 (30)	7 (25)	7 (21.9)	16 (28.1)	19 (43.2)	0.28
Cholecalciferol use (no. [%])	28 (46.7)	11 (39.3)	9 (28.1)	28 (49.1)	19 (43.2)	0.37
Ergocalciferol use (no. [%])	2 (3.3)	1 (3.6)	2 (6.3)	0 (0)	2 (4.5)	0.53
Calcitriol use (no. [%])	1 (1.7)	0 (0)	1 (3.1)	10 (17.5)[ii]	6 (13.6)	0.005
Body mass index (kg/m²)	27.9±6.5	27.5±7.9	30.3±6.4	32.0±7.7	29.9±7.4	0.55
Systolic blood pressure (mmHg)	124±17	127±16	128±20	132±17	131±18	0.63
Hemoglobin (g/dL)	12.8±1.5	12.0±1.8	12.0±1.7	11.8±1.5[ii]	10.9±1.4[iii]	0.007
Fasting plasma glucose (mg/dL)	106±20	110±25	112±36	119±31	125±45	0.06
Blood urea nitrogen (mg/dL)	17±6	21±5	30±11[ii]	42±13[iii]	53±19[iii]	<0.001
Serum creatinine (mg/dL)	0.9±0.2	1.3±0.2	1.6±0.3[ii]	2.7±0.7[ii]	6.3±2.5[iii]	<0.001
Estimated GFR (mL/min/1.73 m²)	80±15	51±5	37±5[ii]	22±4[ii]	9±3[iii]	<0.001
Serum sodium (mEq/L)	141±3	141±2	141±4	141±2	140±4	0.37
Serum potassium (mEq/L)	4.3±0.4	4.6±0.6	4.6±0.5	4.7±0.5[i]	4.8±0.6[i]	0.006
Serum chloride (mEq/L)	103±2	103±2	104±4	104±3	100±7[i]	0.008
Serum bicarbonate (mEq/L)	25±2	25±2	24±3	24±3	23±4	0.14
Corrected serum calcium (mg/dL)	9.5±0.5	9.4±0.4	9.4±0.5	9.4±0.4	9.3±0.5	0.47
Serum phosphate (mg/dL)	3.3±0.4	3.3±0.7	3.5±0.6	4.0±0.6[ii]	5.1±1.0[iii]	0.003
Serum alkaline phosphatase (U/L)	79±27	74±37	100±115	92±34	100±63	0.23
Serum albumin (g/dL)	4.2±0.4	4.1±0.3	4.2±0.3	4.1±0.3	4.1±0.4	0.12

Kritmetapak et al. Page 20

Characteristics	Estimated GFR (mL/min/1.73 m²)					P for trend
	>60 (n = 60)	45–59 (n = 28)	30–44 (n = 32)	15–29 (n = 57)	<15 (n = 44)	
24-hour urine protein (mg/day)	216 (153–355)	201 (133–397)	289 (165–557)	629 (315–2,768)[i]	2,861 (1,754–4,283)[iii]	0.009
Serum intact PTH (pg/mL)	63 (47–85)	66 (45–83)	72 (46–93)	115 (92–168)[ii]	246 (143–393)[iii]	0.006
Serum 25(OH)D (ng/mL)	38.8±11.9	49.9±12.3	37.1±11.9	42.2±13.0	41.8±15.7	0.14
Serum 1,25(OH)$_2$D (pg/mL)	41.5±12.7	33.5±12.5[i]	29.8±11.6[i]	21.7±8.4[ii]	15.6±1.8[iii]	0.005
Serum intact FGF23 (pg/mL)	41.9 (33.1–47.4)	56.4 (47.4–58.6)	62.9 (53.2–75.6)	117.5 (87.6–137.2)[iii]	327.5 (195.1–456.3)[iii]	<0.001

For normally distributed continuous variables, mean±SD; for non-normally distributed continuous variables, median (interquartile range); for categorical variables, N (%).

[i-iii] Compared with patients with eGFR >60 mL/min/1.73 m²:

[i] $P < 0.05$;

[ii] $P < 0.01$;

[iii] $P < 0.001$.

FGF23, fibroblast growth factor 23; 25(OH)D, 25-hydroxyvitamin D; 1,25(OH)2D, 1,25-dihydroxyvitamin D.

Table 2.

Serum concentration of LC-HRMS PTH1–84 and PTH fragments according to stages of renal function.

PTH peptides	All	Estimated GFR (mL/min/1.73 m^2)						P for trend
		>60	45–59	30–44	15–29	<15		
PTH1–84	82 (66–120)	70 (67–95)	72 (58–93)	76 (61–95)	77 (58–93)	115 (81–189)[ii]		0.008
PTH28–84	75 (56–118)	55 (49–70)	58 (58–141)	68 (61–111)	71 (49–96)	112 (80–180)[iii]		0.009
PTH34–77	113 (68–307)	59 (45–78)	56 (47–66)	109 (97–125)	114 (88–134)[ii]	285 (194–393)[iii]		0.004
PTH34–84	219 (97–554)	99 (67–213)	165 (81–413)	206 (93–298)[i]	231 (149–362)[i]	1,026 (480–1,498)[iii]		0.006
PTH37–77	206 (99–349)	105 (96–181)	103 (82–179)	116 (50–227)	140 (95–206)[i]	345 (206–483)[iii]		0.008
PTH37–84	126 (64–327)	69 (54–122)	77 (52–184)	84 (65–175)	121 (76–224)[i]	456 (236–771)[iii]		0.006
PTH38–77	177 (91–605)	72 (53–123)	124 (77–221)	133 (77–235)	140 (87–289)[i]	901 (337–2,147)[iii]		0.008
PTH38–84	80 (39–206)	35 (25–61)	45 (29–81)	48 (32–83)	53 (35–109)	265 (104–429)[ii]		0.009
PTH4S-84	153 (110–277)	132 (95–158)	125 (74–165)	135 (108–159)	140 (98–156)	381 (215–587)[iii]		0.005

Values are shown as median (interquartile range, pg/mL).

[i-iii] Compared with patients with eGFR >60 mL/min/1.73 m^2:

[i] $P < 0.05$;

[ii] $P < 0.01$;

[iii] $P < 0.001$.